NANO LETTERS

2008
Vol. 8, No. 2
611−618

Soft Patchy Nanoparticles from Solution-Phase Self-Assembly of Binary Diblock Copolymers

Goundla Srinivas and Jed W. Pitera*

IBM Almaden Research Center, 650 Harry Road, San Jose, California 94086

Received November 20, 2007; Revised Manuscript Received December 20, 2007

ABSTRACT

The fabrication of highly ordered, defect-free nanostructures is a key challenge in nanotechnology. Bottom-up fabrication approaches require nanobuilding blocks of precisely defined size and shape. In this work we propose a simple approach to obtain one type of building block—soft patchy nanoparticles—suggested by a series of coarse grain molecular dynamics simulations. A binary mixture of two different diblock copolymers with a common hydrophobic block but sufficiently dissimilar hydrophilic blocks reliably self-assembles into a "patchy" spherical micelle in water, with phase separation of the two hydrophilic blocks on the surface of the micelle core. Subsequent crosslinking of the core to solidify the patchy sphere geometry should allow further hierarchical assembly. Altering the hydrophilic versus hydrophobic composition of each polymer yields a change of morphology from "patchy spheres" to "patchy cylinders". Furthermore, by controlling the interaction strength of the blocks with solvent, the patches can be selectively placed either on the outer surface or inside the core of the micelle. The number and size of the patches are found to be largely controlled by the composition of the binary copolymer mixture.

A key goal of nanotechnology is the fabrication of complex, highly ordered, defect-free structures on the nanometer scale. Continued advances in areas such as electronics and photonics depend on the ability to manufacture ever-smaller nanostructures reliably and cost-effectively. As traditional top-down approaches like optical lithography approach their intrinsic feature size limits, bottom-up self-assembly is emerging as a promising alternative.[1,2] Bottom-up approaches start with well-defined, highly uniform building blocks, including rigid molecules,[3] nanoparticles,[4] polymers,[5] or colloids.[6] These building blocks can then self-assemble into the desired structure of interest, with the driving forces for self-assembly coming from interparticle interactions, possibly modulated by external fields. However, synthesizing such building blocks poses a tremendous challenge.

In a pioneering experimental study Pine et al.[6] successfully obtained well-defined polyhedral geometries using colloidal spheres driven to associate by capillary forces. A richer variety of self-assembled structures can be constructed if the particles are "decorated" with specific, anisotropic interparticle interactions.[7−9] Glotzer et al.[7] introduced a "patchy-particle" model to study the self-assembly of ordered 2D and 3D objects. By selecting the starting particle size and shape as well as the number and position of the "patches", they could successfully self-assemble complex structures including sheets, spheres, and pyramids.[10]

Unfortunately, such precisely controlled building blocks are not always readily available at the nanoscale, so a wide variety of preparation approaches have been attempted. Biologically inspired examples include biomolecular−inorganic hybrid nanobuilding blocks,[11−14] quantum dots ordered by genetically engineered viruses,[13] and specific 3D patterns of gold nanoparticles on the surface of cowpea mosaic viruses (CPMV).[12] Other approaches use microphase separation of surface ligands[15] or block copolymers[16−19] deposited as a thin film on the surface of a predefined nanoparticle.

Most of the structures that involve nonbiological materials result from the assembly of microspheres or colloidal particles. There is no experimental study to date that reports the self-assembly of nanoscale patchy particles in a single step. Similarly, contemporary theoretical and computational studies involve "prebuilt" patchy particles composed of soft or hard spheres[7,20] and rarely address this synthesis problem. In this study we report on a potential novel route to "patchy particles" (both spheres and cylinders) via the self-assembly of a simple binary mixture of diblock copolymers in solution. This idea was suggested by a series of coarse-grain (CG) molecular dynamics (MD) simulations. Our simulations indicate that a mixture of AB and CB diblock copolymers with properly chosen monomers should self-assemble in solution to form "patchy" spherical or cylindrical micelles with the patches formed by the C block (shown in Figure 1). The micelle size is governed by the block copolymer chain lengths and can be relatively uniform (∼6 nm).[21] Patch formation is driven by the immiscibility of the A and C surface blocks as well as the differential surface curvature

* Corresponding author. E-mail: pitera@us.ibm.com.

10.1021/nl073027q CCC: $40.75
Published on Web 01/12/2008

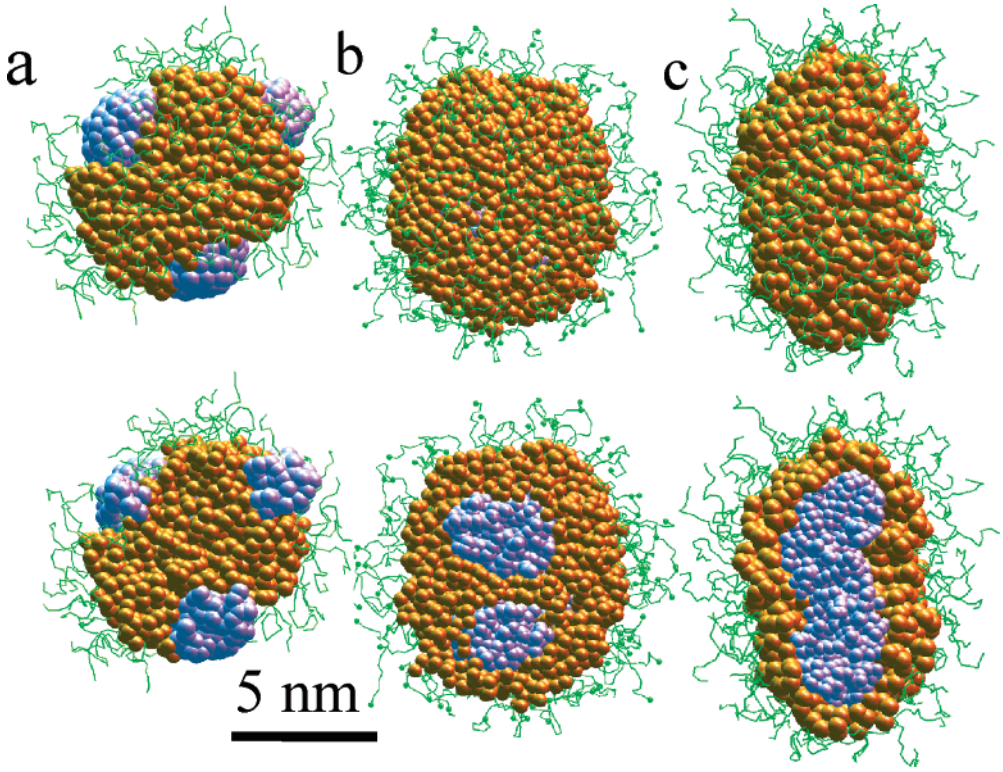

Figure 1. (a) Self-assembled "spherical patchy micelle" from a binary mixture of $A_{13}B_7$ and $C_{13}B_7$ copolymers in water as observed in CG-MD simulations. "C" segments aggregate to form patches on the surface of "B" core. A cross-sectional view (bottom) is also shown. (b) Spherical micelle formed from a binary mixture of $A_{13}B_7$ and $C^w_{13}B_7$ copolymers self-assembling in water. A cross-sectional view revealing the arrangement of patches confined within the micelle is shown below. (c) Spherical micelle self-assembled from an $A_{16}B_4$ and $C^w_{16}B_4$ binary mixture in water. Cross-sectional view (bottom) reveals a concentric dual-core micelle conformation. Color scheme: A (green), B (brown), and C or C^w (blue). "A" segments are shown as lines, while all others are spheres. Water is omitted for clarity.

of the A and C patches. Since amphiphiles at high concentrations rearrange from micellar structures to more complex ordered phases,[22] the assembled particles would most likely need to be fixed in their patchy particle geometry by crosslinking of the core (e.g., UV crosslinking of polystyrene or similar strategies) prior to the next stage of self-assembly.

Block copolymer self-assembly involves long time and length scales which put this problem beyond the scope of detailed atomistic simulations. On the other hand, analytic or mean field calculations may provide a broader picture but can omit details crucial to the self-assembly mechanism. Hence, we have adopted an intermediate coarse-grain (CG) methodology.[23,24] CG molecular dynamics (CGMD) is fast enough to simulate the large length and time scales involved in such problems while preserving the structure and geometry of individual molecules. Previous studies have emphasized both the advantages of CGMD in studying the self-assembly of lipids[25,26] and polymers[27,28] and other macromolecular phenomena.[29,30]

We studied the self-assembly of a number of different binary mixtures of two model block copolymers, namely A_xB_y and C_iB_j (or $C^w_iB_j$) using CGMD simulations. Each copolymer was at least 20 monomers long and composed of an A, C, or C^w block and a hydrophobic (B) block. The typical simulation system contained a total of 250 copolymers in 25 000 CG waters (~75 000 water molecules). The force field function and parameters for the block copolymers and solvent were similar to those from our previous study.[27] One of the block copolymers in this study was generated from the previously parametrized polyethyleneoxide−polyethylethylene (PEO−PEE) diblock copolymer. For generality, we denote this as an A_xB_y copolymer (x and y represent the number of repeating units in polymer segments A and B, respectively). Each monomer unit of either polymer block was represented by a single spherical CG unit (A for EO and B for EE). The CG polymer was constructed by connecting the consecutive center of masses of the corresponding all-atom structure by harmonic bond potentials of the form, $U_{bond}(r_{ij}) = (k_b/2)\,(r_{ij} - r_o)^2$, where r_o is the equilibrium bond distance, the distance between bonded CG particles is denoted by r_o, and k_b is the bond stretching force constant. The bond angle between three connected sites was similarly harmonic, $U_{bend}(\theta_{ijk}) = (k_\theta/2)\,(\theta_{ijk} - \theta_o)^2$, where θ_{ijk} is the bond angle formed by sites i, j, and k, and θ_o is the equilibrium bond angle. For the nonbonded interaction, most pair interactions employed a potential of the form[31]

$$U(r_{ij}) = (27/4)\epsilon[(\sigma/r_{ij})^m - (\sigma/r_{ij})^n] \qquad (1)$$

where, for the values of m and n used here, ϵ and σ represent the well-depth and van der Waals diameter of the corresponding species, respectively (Table 1). For the interaction between CG water particles, $m = 6$ and $n = 4$. All other

Table 1. Interaction Parameter Strengths (ϵ_{ij}) between Various CG Units Constituting the Copolymers Used in This Study Are Listed below ("*tab*" Represents the Tabulated Potential)

ϵ_{ij}	A	B	C	C^w	W
A	tab	90	20	20	tab
B	90	170	90	90	193
C	20	90	360	360	tab
C^W	20	90	360	360	40
W	tab	193	tab	40	212

nonbonded interactions, including those between polymer and CG water (denoted by W), used $m = 9$ and $n = 6$. The three nonbonded interaction pairs (A−A, A−W, and C−W) not listed in Table 1 were treated with tabulated potentials developed previously.[28] These interactions are complex due to the polar nature of the atoms present and hence could not be modeled by the simple form of eq 1. The nonbonded interactions were smoothly switched off at a cutoff distance of 1.4 nm. There are no explicit electrostatic interactions in the model. We have previously estimated the effective Flory−Huggins parameter (χ) for the A−B interaction as 3.2 or greater.[32]

We also modified the interaction potential of one of the monomers (A) to generate two additional monomer types C and C^w, as well as block copolymers C_xB_y and $C^w_xB_y$. A and C are purely hydrophilic, and B is fully hydrophobic. However, we distinguished C from A by making the C−C interaction highly favorable ($\epsilon_{C-C} = 360$ kcal/mol) and weakening the C−A interaction ($\epsilon_{C-A} = 20$ kcal/mol). The C^w monomer type is similar to C, except that it also repels the solvent ($\epsilon_{CW-C} = 40$ kcal/mol). Note that C and C^w represent model polymers as their parameters are not based on any particular monomer chemistry. A similar strength of the C−C or C^W−C^W interaction, however, would probably only be achievable in a real system through ion−ion or metal−ligand interactions.

We used the cm3d package[33] to carry out the simulations on 64 to 128 processors of an IBM Blue Gene/L system. All simulations were carried out in the NPT ensemble ($T =$ 298 K, $P = 1$ atm) with independent scaling of each of the three box edge lengths and a 10 fs time step. Nose−Hoover extended systems[34] were used for temperature and pressure control.[35] In general, the effective CG simulation time scales are typically 2 orders of magnitude larger than those of their all-atom counterparts.[36] In other words, the CG simulations explore conformational space more quickly than implied by the nominal simulation time. Nevertheless, all the simulation times reported in this article are the real simulation times, not the scaled effective CG times. Separate simulations have been carried out to determine the composition phase diagram for AB or BC block copolymers in water by varying the A/B or C/B ratio. In both polymers, spherical micelle formation is preferred when the fraction of B monomers (f_B) is less than 0.4, while $0.4 < f_B < 0.6$ results in a cylindrical morphology.

In order to explore the self-assembly of binary block copolymer mixtures and study patchy particle formation, we constructed various systems with differing B fractions. Details of all the systems studied are presented in the Supporting Information. In the following, we describe the systems that are most relevant in the present context. Initially, a 1:1 mixture of spherical micelle forming diblock copolymers $A_{13}B_7$ and $C_{13}B_7$ ($f_B = 0.35$) were randomly dispersed in water in a cubical simulation box with a volume of 2744 nm^3. We followed the self-assembly for 50 ns after an initial equilibration. In the initial stages of self-assembly, the diblock copolymers started forming small aggregates of similar entities (e.g, $(A_{13}B_7)_m$ or $(C_{13}B_7)_n$), which gradually grew in size with time. Mutual fusion took place by random encounters with other aggregates. While the fusion between aggregates of the same species ($(A_{13}B_7)_m + (A_{13}B_7)_n$ or $(C_{13}B_7)_m + (C_{13}B_7)_n$) is straightforward, the fusion between dissimilar aggregates ($(A_{13}B_7)_m + (C_{13}B_7)_n$) is complex. This may be due to the strong repulsion between the A and C blocks forming the outer shell of the aggregates. The fusion itself appears to be driven by the favorable burial of B blocks. Once the aggregates started fusing, the hydrophobic (B) blocks from both species rapidly mixed to form the core of the resulting micelle, while both A and C blocks constituted the outer shell. However, the unfavorable interactions between A and C monomers drive them to form individual domains on the surface of the micelle. Since C−C self-interactions are stronger than C−water interactions, the C segments collapse to form patchlike structures on the outer surface of the B core, while the highly hydrophilic A blocks remain swollen by solvent. The later stage self-organization among A and C blocks resulted in the formation of "patchy micelles" or "patchy spheres" in which C segments formed patches on the surface of the spherical micelle. The smaller C patches gradually aggregated and increased in size. The long-time kinetics of this fusion process is relatively slow. One such "patchy-sphere" observed in CG simulations is shown in Figure 1a. Note that it is entirely composed of diblock copolymers without a rigid core—a "soft patchy sphere".

The interaction details and relative lengths of the segments constituting the block copolymers were found to greatly influence the outcome of the self-assembly. For instance, altering the interaction between C and water to be less favorable, thereby making C relatively hydrophobic (C^w), caused the patches to move from the outer surface to inside the hydrophobic core (Figure 1b). The C^w segments form individual clusters as before but inside the core of the spherical micelle. Increasing the fraction of C^w led to a morphology where the individual patches fuse inside the core (Figure 1c). In this case, the C^w segments are long enough to interpenetrate across the patches, thereby inducing fusion within the core and forming a multicore (B−C^W−A) spherical micelle. In order to verify the robustness of these simulations to system size effects, we also carried out simulations with a larger system size and different initial configuration (three systems with 320 $A_{13}B_7$ and $C_{13}B_7$ copolymers in 32 000 CG waters; see Supporting Information), which also resulted in the formation of a patchy spherical micelle.

Additionally, simultaneous segment length variation within the AB and BC copolymers resulted in the formation of

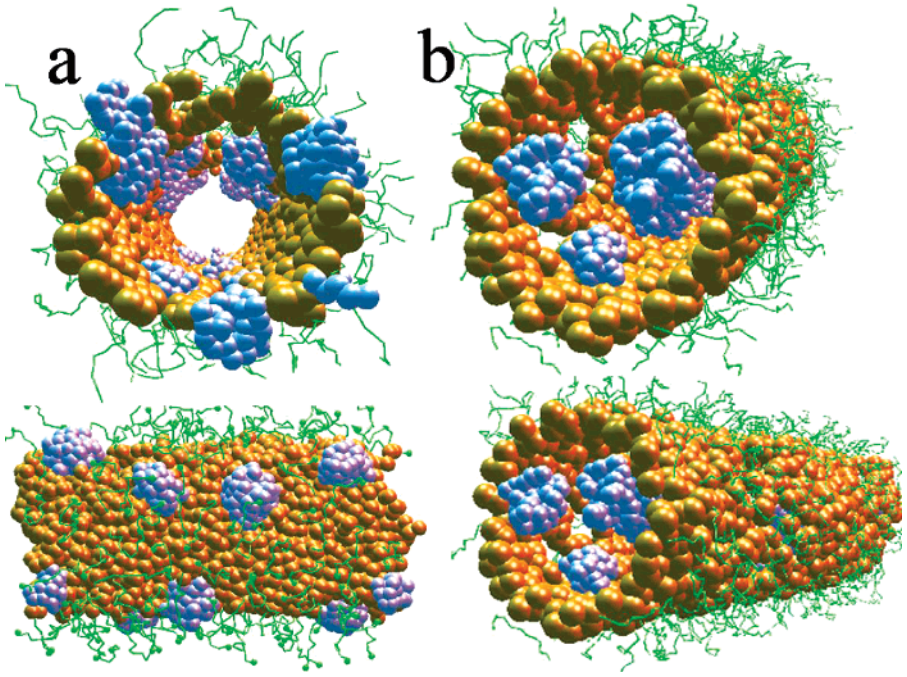

Figure 2. (a) Cylindrical micelle obtained from the self-assembly of a copolymer mixture $A_{13}B_7$ and C_7B_{13} in water (front view). To illustrate the cylindrical geometry, only B monomers within a distance of 0.5 nm from the cylindrical surface are shown. A side view revealing the "patchy cylinder" is shown in the bottom panel. (b) Formation of cylindrical micelle from an $A_{13}B_7$ and $C_7^wB_{13}$ copolymer mixture in water. In this case, the C segments form "patches" within the cylinder, not on the surface. The color code is the same as that in Figure 1.

nonspherical morphologies. The same initial configuration that yielded "patchy spheres" self-assembled to a "patchy-cylinder" morphology (Figure 2a) when the B content in the copolymer mixture was increased by 15% ($A_{13}B_7 + C_7B_{13}$). As before, C segments formed isolated patches on the outer surface of the cylindrical core formed by B. Upon changing the nature of C segments to relatively hydrophobic (C^w), this mixture self-assembled to a cylindrical micelle with the C^w patches buried inside the cylinder (Figure 2b).

A simple agglomerative clustering algorithm was used to follow the process of cluster formation during the block-copolymer self-assembly. In Figure 3a, we plot the number of BC clusters as a function of simulation time during the self-assembly of a spherical patchy particle. Two BC copolymers were considered to be part of the same cluster if any of the CG particles of each molecule were within 0.9 nm of each other. Isolated molecules were counted as belonging to their own cluster. As can be seen from the figure, the cluster population shows an initial rapid decay followed by a slow long-time relaxation tail. Such behavior has been observed in lipid vesicle budding and fission processes as well.[37,38] In the same figure, the size of the biggest BC cluster is also plotted as a function of time.

We proceeded to examine the relative size distribution of the patches on the micelle surface from each simulation. The number of copolymers forming a patch was determined by averaging the cluster statistics from the final 100 snapshots of the respective simulation. Figure 3b shows the relative sizes of each patch present on the micelle surface, for three different simulations where a spherical micelle with four patches was observed. The significant deviation from uniform patch sizes suggests that our calculations may not be fully equilibrated. An alternative explanation is that the patch size is subject to significant fluctuations, even at equilibrium, and further simulation and modeling are necessary to differentiate these hypotheses. As can be seen from the figure, similar results were obtained by varying segment lengths of A and C. The final snapshots and corresponding pie charts showing relative patch distribution in each case are also shown in the same figure.

In order to examine the stability and energetics of patch formation, we carried out a separate simulation with a preassembled patchy micelle in water. The patchy micelle was constructed such that the right half of the micelle was fully made of $A_{13}B_7$ copolymers while the other half was made of $C_{13}B_7$ (Supporting Information, Figure S5). This initial configuration started rearranging, accompanied by a gradual decrease in energy, as the simulation began. The rearrangement process finally resulted in a patchy micelle in which the C blocks formed well separated finite sized patches (Figure S5b). The formation of these finite size patches is energetically favored (as shown in Figure S5c).

All the results presented above were obtained with a 1:1 mixture of AB and BC copolymers. However, the relative composition of individual species plays an important role in determining the properties of binary mixtures.[39] Consequently, we studied the composition dependence of patch formation. For this purpose, we selected $A_{13}B_7 + C_{13}B_7$ copolymer mixtures with a total of 160 copolymers. We varied the number of $C_{13}B_7$ copolymers from 0 to 160 while keeping the total number of copolymers in the system

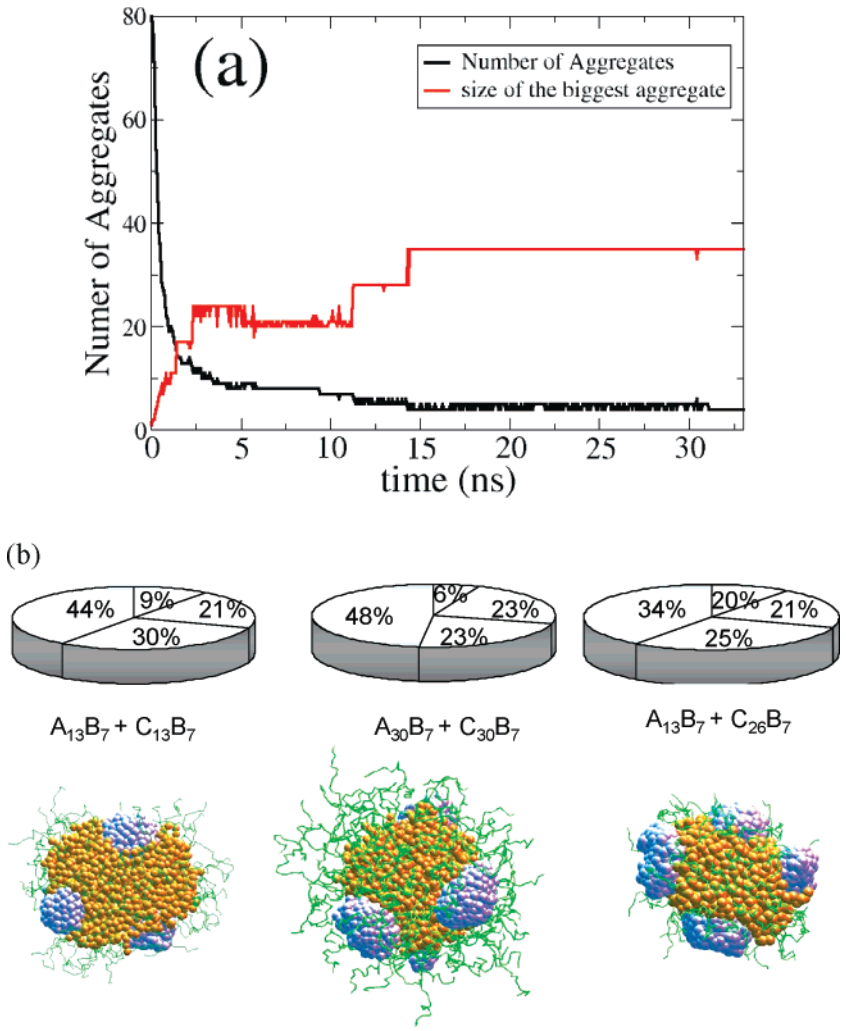

Figure 3. (a) The number of BC copolymer aggregates is plotted as a function of simulation time during the self-assembly of $A_{13}B_7$ and $C_{13}B_7$ in water. The evolution of the biggest cluster is also shown. (b) Pie charts showing the percentage of BC copolymers in each patch for three different block copolymer mixtures. Four patches are formed in each case. The final snapshots obtained from each simulation are shown below the pie charts, using the same coloring scheme as that in Figure 1.

constant to generate nine different systems corresponding to different $C_{13}B_7$ compositions (note that the number of water molecules remains constant in all the systems. Hence, for simplicity we chose mole fraction notation to represent the relative content of corresponding block copolymer alone). For example, a system with a $C_{13}B_7$ mole fraction $X_{CB} = 0.25$ contained 40 $C_{13}B_7$ and 120 $A_{13}B_7$ copolymers (Table 2). The final snapshots observed in all nine systems corresponding to different mole fractions are shown in Figure 4a. Regardless of the number of $C_{13}B_7$ copolymers present in the system, self-assembly in all cases resulted in the formation of a spherical micelle, suggesting that the morphology of the system is indeed determined by the relative volume fraction of (A + C) and B blocks. A pure $A_{13}B_7$ copolymer system ($X_{CB} = 0$) yielded a plain spherical micelle without any patches. Patches start forming with the addition of $C_{13}B_7$ copolymers as shown in the figure. The number of patches is found to be roughly proportional to the $C_{13}B_7$ mole fraction (Figure 4b). The size of micelle is estimated using the core density distributions (averaged over the last 5 ns). On going from $X_{CB} = 0$ to $X_{CB} = 1$, we observe that the size of the micelle core did not change by more than 6% (Supporting Information).

Table 2. Compositions of Nine Different Systems with Different Copolymer Mole Fractions Simulated in This Study[a]

X_{AB}	X_{CB}	N_{AB}	N_{BC}
1.000	0	160	0
0.875	0.125	140	20
0.75	0.25	120	40
0.625	0.375	100	60
0.5	0.5	80	80
0.375	0.625	60	100
0.25	0.75	40	120
0.125	0.875	20	140
0.0	1.0	0	160

[a] Each system contains a total of 160 copolymers and 16 000 CG water molecules. N_{AB} and N_{CB} represent the number of $A_{13}B_7$ and $C_{13}B_7$ copolymers, respectively.

As before, we studied the dynamics of $C_{13}B_7$ aggregate formation. In all the cases the aggregation is faster at short times, which is followed by a slow long time tail as shown

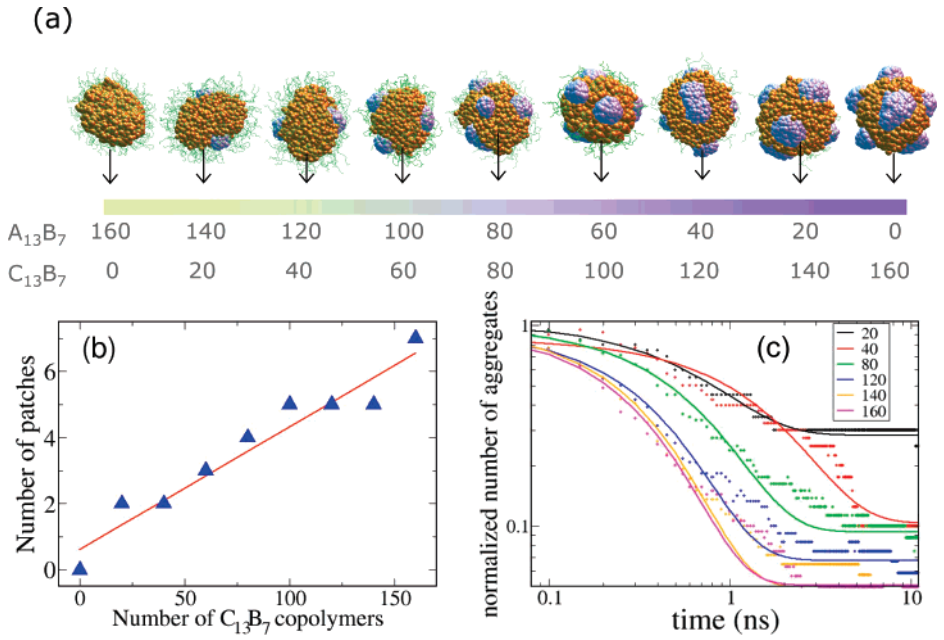

Figure 4. (a) Micelle structures obtained from the self-assembly of $A_{13}B_7$ and $C_{13}B_7$ in water at nine different binary compositions. The number of $A_{13}B_7$ and $C_{13}B_7$ copolymers corresponding to the binary composition is shown below each structure. (b) The number of patches as a function of the $C_{13}B_7$ copolymer compostion of the micelle. (c) The number of BC copolymer aggregates (normalized by the number of patch forming ($C_{13}B_7$) copolymers) as a function of time for different BC compositions. Lines represent fits to eq 3.

in Figure 4c. Nevertheless, the number of $C_{13}B_7$ aggregates was found to decrease more rapidly with increasing $C_{13}B_7$ mole fraction. The simulation results are found to roughly fit the following empirical formula

$$C_n(t) = a_0 + a_1 \exp(-a_2 t) \tag{3}$$

where the constants a_0, a_1, and a_2 depend on the system and the block copolymer composition.

In the following we suggest a possible mechanism for the patchy particle formation. A simulation with 160 $A_{13}B_7$ copolymers in 16 000 CG waters (pure $A_{13}B_7$ system) showed that the self-assembly in this case results in the formation of a spherical micelle (shown in Figure 5a). The B blocks constitute the core, while the A blocks forming the shell are fully solvated by the water. The spherical micelle can be viewed as a sphere made of several wedge-shaped copolymer aggregates each with positive interfacial curvature, as shown in Figure 5a. Similarly, pure $C_{13}B_7$ block copolymers self-assemble to a spherical micelle in water (Figure 5b). However, in this case, the C blocks form patches on the outer surface of the micelle core. We examine this conformation by randomly selecting a patchy domain. Interestingly, the CB block copolymers also aggregate to form a wedge-shaped structure (shown in Figure 5b), but one with negative interfacial curvature as opposed to the positively curved wedge in the case of $A_{13}B_7$ diblock copolymers. In the case of an $A_{13}B_7$ and $C_{13}B_7$ binary mixture, the initial stages of self-assembly result in the formation of both positively curved ($A_{13}B_7$) and negatively curved ($C_{13}B_7$) wedge-shape aggregates. One of the energetically favored structures that can efficiently accommodate both the positively and negatively curved wedge-shape aggregates is a patchy micelle. The formation of a patchy micelle from both positively and negatively curved wedges is schematically shown in Figure 5c.

Uniformity of the nanoscale building blocks is critical for any bottom-up manufacturing approach based on such soft "patchy" particles. In the case of the spherical micelles considered here, there are three critical areas of variation between individual micelles: the size of each micelle (a function of the number of copolymers forming the micelle), the number and nature of patches (dependent on the AB/CB ratio), and the relative placement of the patches on the surface of the particle. If the micellar self-assembly takes place near the critical micelle concentration, the distribution of the number of chains in each micelle is expected to have a relative fwhm of 5−15% of the average number of chains per micelle.[40] This means that 95% of micelles will fall within ±12% of the average number of chains. This number variation implies a variation in the radius of the micelle of ±4%. For some applications, such as photonic crystals, where long-range crystalline order is desired, the maximum useful variation in the particle radius is estimated to be ∼3−5%.[41] In these cases it may be necessary to employ a further separation or purification step to narrow the micelle size distribution in order for these building blocks to be useful. As seen above, the number and distribution of patches appears to be straightforwardly dependent on the AB/CB composition of the micelle, so careful control of the parent mixture will be necessary to yield micelles with the desired number of patches. The systematic dependence of patch number on composition seen in Figure 4b suggests that fluctuations play a limited role in defining the number of

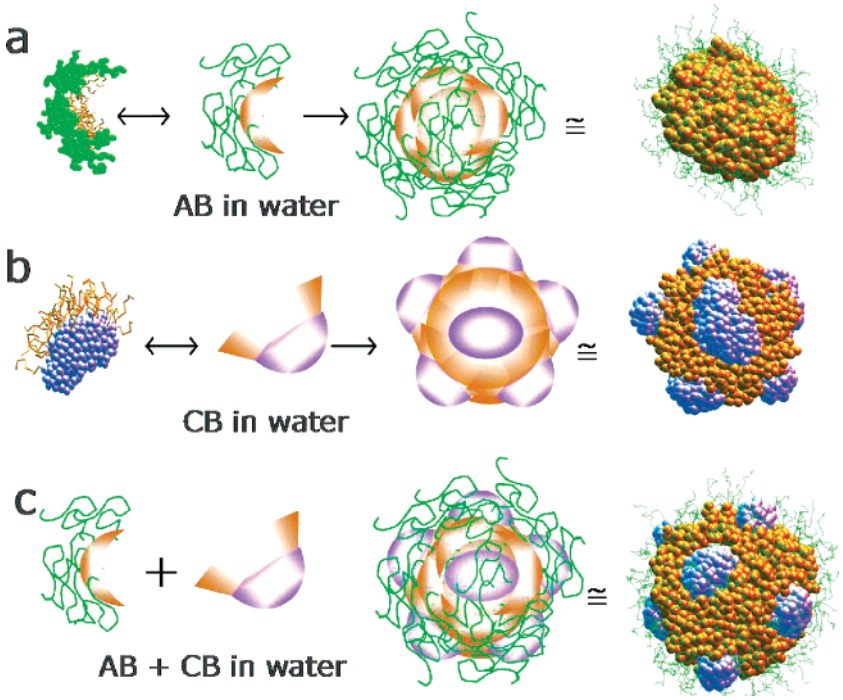

Figure 5. (a) Schematic representation of the positive surface curvature of AB diblock copolymers and corresponding simulated AB micelle. (b) Illustration of the negative surface curvature observed for CB patches in a pure CB micelle. (c) A possible mechanism for patch formation showing the assembly of both positively and negatively curved wedge-shaped aggregate assembly to form a patchy micelle. In each case, the corresponding simulation snapshot is shown in the right-hand column.

patches at equilibrium, though that remains a possibility. Fluctuations may also affect the relative patch sizes more than their number. Regarding the spatial distribution of patches, we have analyzed the distribution of angles between patches observed in our simulations and find that it is dependent on the number of patches on the micelle. Micelles with two patches show an interpatch angle distribution with a maximum at roughly 170 ± 5°; those with three patches, 120 ± 7.5°; and those with four patches, 105 ± 10°. The micelles with five patches show a multimodal angle distribution with maxima at 80°, 120°, and 160°. These correspond well with the idealized geometries of 180°, 120°, 109.5° and (90°, 120°, 180°), respectively. Details of the calculation and a graph of the distributions are included in the Supporting Information.

In conclusion, our simulations suggest that a binary mixture of appropriately chosen chemically distinct copolymers should selectively self-assemble into "patchy particle" micelles. After stabilization by crosslinking or fixation of the hydrophobic core, these "patchy particles" could self-assemble into more complex structures. The micelle size is well controlled by the polymer length,[21] while the number and size of the patches will be a function of composition as well as the line tension between A and C blocks, as with binary lipid vesicles.[42] A more detailed study of the accessible patch numbers, sizes, and geometries is still necessary. Once these details are addressed, our approach may represent a useful route to synthesize nanoscale "patchy particles" for subsequent self-assembly into more complex structures. Furthermore, we have shown that tuning the copolymer chemistry also allows "patchy cylinders" and "multicore" cylindrical conformations to be obtained. We envisage such multicore assemblies will be of great potential in many chemical and biological applications including molecular transport and drug delivery.

Supporting Information Available: Details of the simulation parameters and methods used as well as additional simulation analyses. This material is available free of charge via the Internet at http://pubs.acs.org.

References

(1) Whitesides, G. M.; Boncheva, M. *Proc. Natl. Acad. Sci. U.S.A.* **2002**, *99*, 4769.
(2) Murphy, C. J. *Science* **2002**, *298*, 2139.
(3) Pan, B. F.; Ao, L. M.; Gao, F.; Tian, H. Y.; He, R.; Cui, D. X. *Nanotechnology* **2005**, *16*, 1776.
(4) Song, T.; Dai, S.; Tam, K. C.; Lee, S. Y.; Goh, S. H. *Langmuir* **2003**, *19*, 4798.
(5) Murray, C. B.; Kagan, C. R.; Bawendi, M. G. *Ann. Rev. Mater. Sci.* **2000**, *30*, 545.
(6) Manoharan, V. N.; Elsesser, M. E.; Pine, D. J. *Science* **2003**, *301*.
(7) Zhang, A.; Glotzer, S. C. *Nano Lett.* **2004**, *4*, 1407.
(8) Bianchi, E.; Largo, J.; Tartaglia, P.; Zccareli, E.; Sciortino, F. *Phys. Rev. Lett.* **2006**, *97*, 168301.
(9) Kern, N.; Frenkel, D. *J. Chem. Phys.* **2003**, *118*, 9882.
(10) Glotzer, S. C.; Solomon, M. J. *Nat. Mater.* **2007**, *6*, 557.
(11) Mirkin, C. A.; Letsinger, R. L.; Mucic, R. C.; Storhoff, J. J. *Nature* **1996**, *382*, 607.
(12) Blum, A.; Soto, C. M.; Wilson, D.; Cole, J. D.; Kim, M.; Gnade, B.; Chatterji, A.; Ochoa, W. F.; Line, T.; Johnson, J. E.; Ratna, B. R. *Nano Lett.* **2004**, *4*, 867.
(13) Lee, S.-W.; Mao, C.; Flynn, C. E.; Belcher, A. M. *Science* **2002**, *296*, 892.
(14) Braun, P. V.; Osenar, P.; Tohver, V.; Kennedy, S. B.; Stupp, S. I. *J. Am. Chem. Soc.* **1999**, *121*, 7302.
(15) Jackson, A. M.; Hu, Y.; Silva, P. J.; Stellacci, F. *J. Am. Chem. Soc.* **2006**, *128*, 11135.
(16) Li, G.; Shi, L.; Ma, R.; An, Y.; Huang, N. *Angew. Chem., Int. Ed.* **2006**, *45*, 4959.
(17) Zheng, R.; Liu, G.; Yan, X. *J. Am. Chem. Soc.* **2005**, *127*, 15358.

(18) Hui, T.; Chen, D.; Jiang, M. *Macromolecules* **2005**, *38*, 5834.
(19) Nelson, D. R. *Nano Lett.* **2002**, *2*, 1125.
(20) Whitelam, S.; Geissler, P. *cond-mat/0508100* **2005**.
(21) Nagarajan, R.; Ganesh, K. *J. Chem. Phys.* **1989**, *90*, 5843.
(22) Laughlin, R. L. *The aqueous phase behavior of surfactants*; Academic Press: Cambridge, 1994.
(23) Goetz, R.; Gompper, G.; Lipowsky, R. *Phys. Rev. Lett.* **1999**, *82*, 221.
(24) Smit, B.; Hilbers, A. J.; Esselink, K.; Rupert, L. A. M.; Van Os, N. M.; Schlijper, A. G. *J. Phys. Chem.* **1991**, *95*, 6361.
(25) Shelley, J. C.; Shelley, M. C.; Reeder, R. C.; Bandyopadhyay, S.; Klein, M. L. *J. Phys. Chem. B* **2001**, *105*, 4464.
(26) Marrink, S. J.; Mark, A. E. *J. Am. Chem. Soc.* **2003**, *125*, 1114.
(27) Srinivas, G.; Discher, D. E.; Klein, M. L. *Nat. Mater.* **2004**, *3*, 638.
(28) Srinivas, G.; Shelley, J. C.; Nielsen, S. O.; Discher, D. E.; Klein, M. L. *J. Phys. Chem. B* **2004**, *108*, 8153.
(29) Lopez, C. F.; Nielsen, S. O.; Srinivas, G.; De Grado, W. F.; Klein, M. L. *J. Theory Comput.* **2006**, *2*, 649.
(30) Srinivas, G.; Discher, D. E.; Klein, M. L. *Nano Lett.* **2005**, *5*, 2343.
(31) Shelley, J. C.; Shelley, M. Y.; Reeder, R. C.; Bandyopadhyay, S.; Moore, P. B.; Klein, M. L. *J. Phys. Chem. B* **2001**, *105*, 9785.
(32) Srinivas, G.; Swope, W. C.; Pitera, J. W. *J. Phys. Chem. B* **2007**, *111*, 13734.
(33) Moore, P. B.; Klein, M. L. "Implementation of a General Integration for Extended System Molecular Dynamics: Technical Report," University of Pennsylvania, 1997.
(34) Hoover, W. G. *Phys. Rev. A* **1985**, *31*, 1695.
(35) Andersen, H. C. *J. Chem. Phys.* **1980**, *72*, 2384.
(36) Lopez, C. F.; Moore, P. B.; Shelley, J. C.; Shelley, M. Y.; Klein, M. L. *Comput. Phys. Commun.* **2002**, *147*, 1.
(37) Cooke, I. R.; Kremer, K.; Deserno, M. *Phys. Rev. E* **2005**, *72*, 011506.
(38) Sunil Kumar, P. B.; Gompper, G.; Lipowsky, R. *Phys. Rev. Lett.* **2001**, *86*, 3911.
(39) Srinivas, G.; Mukherjee, A.; Bagchi, B. *J. Chem. Phys.* **2001**, *114*, 6220.
(40) Kao, C. R.; de la Cruz, M. O. *J. Chem. Phys.* **1990**, *93*, 8284.
(41) Allard, M.; Sargent, E. H. *Appl. Phys. Lett.* **2004**, *85*, 5887.
(42) Yamamato, S.; Hyodo, S. *J. Chem. Phys.* **2003**, *118*, 7937.

NL073027Q